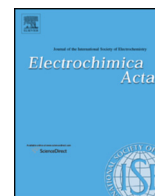Contents lists available at ScienceDirect

Electrochimica Acta

journal homepage: www.elsevier.com/locate/electacta

High Performance Zn/LiFePO$_4$ Aqueous Rechargeable Battery for Large Scale Applications

CrossMark

Nulati Yesibolati [a,b], Nurzhan Umirov [a,b], Aibolat Koishybay [a], Marzhana Omarova [a], Indira Kurmanbayeva [a,b], Yongguang Zhang [a,b,c], Yan Zhao [a,b,c], Zhumabay Bakenov [a,b,*]

[a] Nazarbayev University, 53 Kabanbay Batyr Avenue, Astana 010000, Kazakhstan
[b] Institute of Batteries LLC, 53 Kabanbay Batyr Avenue, Astana 010000, Kazakhstan
[c] Research Institute for Energy Equipment Materials, Hebei University of Technology, Tianjin 300132, China

A B S T R A C T

In this work, a novel aqueous rechargeable battery Zn/LiCl-ZnCl$_2$/LiFePO$_4$ has been developed. The electrochemical performance of olivine LiFePO$_4$ positive electrode has been investigated in the structure of this battery. Along with a high (about 100%) coulombic efficiency, this electrode exhibited enhanced cycling performance at various current densities up to 60 C with the average operation voltage 1.2 V. A capacity of 92 mAh g^{-1} was achieved over 400 cycles at a cycling rate 6 C, and exhibited a superior rate capability with the capacities of 72 mAh g^{-1} at 30 C and 45 mAh g^{-1} at 60 C, respectively. The battery temperature tolerance was first investigated, and it demonstrated a very stable cycling at a wide temperature range from −10 °C to 50 °C. A cylindrical battery with the capacity of 150 mAh was first designed using proposed configuration and successfully operated under 54 mA with high efficiency and capacity retention. Zn/LiFePO$_4$ battery offers an exceptionally safe, low cost, long cycling life, and high energy and power density energy storage for large-scale applications.

© 2014 Elsevier Ltd. All rights reserved.

1. Introduction

Lithium-ion batteries (LIBs) find broad applications as power sources for various devices due to their extraordinary cycling performances and high energy densities [1,2]. However, LIBs have serious issues arising from use of flammable, low conductive and expensive organic electrolytes, which require strictly controlled environment during assembly and production of batteries [2–5], and restricts a wide application of LIBs in large-scale energy storage.

Aqueous rechargeable lithium batteries (ARLBs) with lithium intercalation electrodes (LICs) could be an attractive alternative to make pre-investment gap of LIBs in large-scale energy storages and eliminate safety issues and reduce the production costs [6,7]. Moreover, the fast lithium intercalation/deintercalation in the aqueous electrolyte media, could allow for the operations under high electric current conditions required especially for high power supply [8–10]. Recently, Wu's group reported a coated Li metal issued as negative electrode for an ARLB. Due to the "cross-over"

effect of Li$^+$ in the coating, the ARLB delivers an energy density which is about 80% higher than that for traditional lithium-ion battery [11–13].

In 1994, J. Dahn et al. reported a VO$_2$/LiMn$_2$O$_4$ rechargeable aqueous battery [14]; however, it suffered from a rapid capacity fading upon cycling. Since that, various aqueous systems have been introduced by varying LICs as both positive and negative electrodes [8,9,15–28]. Some suitable positive and negative electrodes for rechargeable batteries are presented in Fig. 1.

Luo reported a LiTi$_2$(PO$_4$)$_3$/LiMn$_2$O$_4$ cell with a capacity of 40 mAh g^{-1} and an energy density of 60 Wh kg^{-1} [19]. Well designed and specially prepared porous LiMn$_2$O$_4$ was investigated by Wu's group [9], and exhibited stable cycling performance upon prolonged operation. These attractive results indicate a great promise for the development of ARLBs for various applications. The electrochemical performance of LiCoO$_2$, LiNi$_{1/3}$Co$_{1/3}$Mn$_{1/3}$O$_2$ in aqueous solution is much dependent on the electrolyte pH due to the competitive lithium and proton intercalation in aqueous systems [10,20,21]. Recently, Cui et al. [22,23] reported a series of metal hexacyanoferrates (M$_x$HCF) with a long cycle life over 40,000 cycles and improved power density.

The olivine structured LiFePO$_4$ is one of the most promising materials for ARLB due to its abundant resources, low cost, high

---

* Corresponding author. Tel.: +7(717)270-65-30.
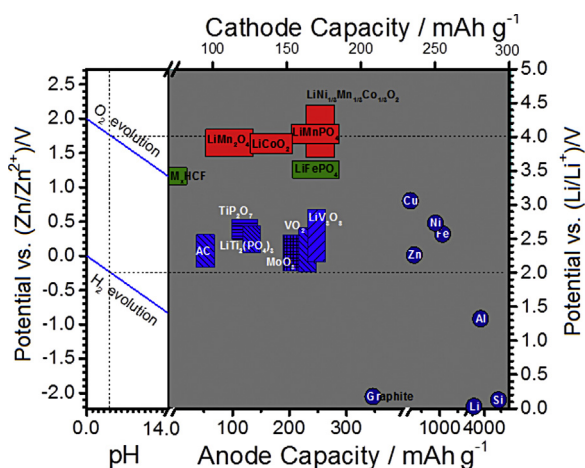 E-mail address: zbakenov@nu.edu.kz (Z. Bakenov).

Fig. 1. Suitable materials for positive and negative electrodes in rechargeable batteries.

thermal, chemical, and electrochemical stability in LIBs [8,24–27]. The LiFePO$_4$ has a pair of redox peaks at 0.495 V and 0.270 V (*vs.* SCE) in a 0.5 M Li$_2$SO$_4$ solution associated with the Li$^+$ insertion/de-insertion in LiFePO$_4$. It is reported that the electrochemical behavior of LiFePO$_4$ in aqueous electrolyte is as same as that in non-aqueous electrolyte, which could be very promising for use in ARLBs [26].

It is reported that in the discharged state, the LICs materials, which are suitable for ARLBs negative electrode by their potentials, would react with water and O$_2$ causing accelerated capacity fading [6]. Furthermore, the low specific capacities of the negative electrodes materials (most reported data are below 250 mAh g^{-1} as shown in Fig. 1) result in low energy and power density. Therefore, the investigation for alternative negative electrodes with high specific capacity and electrochemical/chemical stability for ARLBs is crucial for its practical application.

Zinc is abundant in the nature and possesses a high theoretical capacity (820 mAh g^{-1}) and a low negative potential (−0.762 V *vs.* SHE) [28]. Various rechargeable zinc batteries have been investigated, for instance zinc-air battery [29,30] nickel–zinc battery [31], Zn-Br flow battery [32], silver–zinc battery [33], Zn-Na$_{0.95}$MnO$_2$ [34] *etc.* in aqueous systems. Since its discovery in 2006, a promising aqueous lithium-ion/zinc (Zn/LiMn$_2$O$_4$) rechargeable battery [35] has attracted attentions as a promising ecologically friendly and safe battery [36,37].

Inspired by this fact, and considering known stable performance of LiFePO$_4$ in conventional LIBs, herein, we engineered an aqueous battery with this electrode and examined its performance in a Zn/LiFePO$_4$ cell operating in an optimized Li$^+$/Zn^{2+} binary electrolyte with a pH = 4, which presents a prolonged cycle span as well as a very promising rate capability (up to 60 C). Its temperature performance has been investigated in this work as well. More interestingly, LiFePO$_4$ electrode was also first investigated in a cylindrical large-scale ARLB of the proposed configuration and reported in this work.

2. Experimental

LiFePO$_4$ powder was used as received (Hohsen Co., Japan), and characterized using XRD and SEM as shown in Supplementary Information (SI, Fig. S1 and Fig. S2).

Supplementry material related to this article found, in the online version, at http://dx.doi.org/10.1016/j.electacta.2014.11.168.

LiFePO$_4$ positive electrodes were prepared by mixing 90 wt% LiFePO$_4$ (Hohsen, Japan), 6 wt% polyvinylidene fluoride (PVdF, Kynar, HSV900) as a binder and 4 wt% ketjen black (Ketjen Black International Co., Japan) as a conducting agent in 1-methyl-2-pyrrolidinone (NMP, Sigma-Aldrich). The resultant slurry was coated on a carbon paper (Alfa Aesar Co.), vacuum dried at 70 °C for 2 h and cut into the disks of 6 mm in diameter. The active material loading in the electrodes was about 3–4 mg in Swagelok-cell. Zn foil (Goodfellow, USA) was used as negative electrode. The electrolyte was prepared by dissolving 3 mol dm^{-3} LiCl (Sigma-Aldrich) and 4 mol dm^{-3} ZnCl$_2$ (Sigma-Aldrich) in deionized water and adjusted the solution to a certain pH by titration by 0.05 mol dm^{-3} LiOH (Sigma-Aldrich) or 0.5 mol dm^{-3} HCl (Sigma-Aldrich). AGM (Absorptive Glass Mat NSG Corporation) separator was soaked in the resultant electrolyte and used in the battery. The electrochemical performance of Zn/LiCl-ZnCl$_2$/LiFePO$_4$ battery was investigated using two-electrode Swagelock™-type cells. The cells were tested galvanostatically on a multi-channel battery tester (BT-2000, Arbin Instruments) at various C rates calculated based on the specific capacity of LiFePO$_4$ (1 C corresponds to 170 mA g^{-1}). The test temperature was controlled using an incubator (Eyela 700 W). Cyclic voltammetry (CV) was performed with a VMP3 potentiostat/galvanostat (Bio-Logic Science Instrument Co.) in a two-electrode cell at different sweep rates and potential ranges. All specific capacities are reported per gram of the active material except the large-scale cylindrical battery, where the capacity is provided per an electrochemical cell, i.e. not divided by the mass.

3. Results and discussion

3.1. Electrochemical Characterizations of Zn/LiFePO$_4$

Although the 4 V materials such as LiMn$_2$O$_4$ [9,17,19], LiMnPO$_4$ [18], LiCoO$_2$ [10,15,16] or LiNi$_{1/3}$Co$_{1/3}$Mn$_{1/3}$O$_2$ [20,21] were reported in ARLBs, their potential plateaus in aqueous media are close to water decomposition potential (Electrochemically stability window). Under these conditions, the oxygen evolution along with the dissolution of the metal ions from the positive electrode could not be avoided. In this work, a full cell was constructed using olivine-structured LiFePO$_4$ and zinc metal as positive and negative electrodes, respectfully, and the electrochemical performance and use of the LiFePO$_4$ positive electrode in this system was investigated and optimized. The water stability window is shown in the left side of the diagram in Fig. 1. At pH 4, the O$_2$ evolution potential decreases to 1.75 V *vs.* Zn/Zn^{2+} while, the working voltage of LiFePO$_4$ is around 1.20 V *vs.* Zn/Zn^{2+} which is much safer than that for other intercalating positive materials. The hydrogen evolution drops to −0.24 V *vs.* Zn/Zn^{2+} at pH 4, while the potential of zinc deposition/dissolution during charge/discharge are above this value, which could assist the system to operate successfully. LiFePO$_4$ with suitable electrochemical potential accompanied with the zinc negative electrode could be operated within the electrochemical stability window of water, and could be considered as one of the best electrode pair for ARLBs. The system provides an operating voltage of 1.2 V. The electrochemical mechanism of the Zn/LiFePO$_4$ battery operation is illustrated in Fig. 2. During the charge process, at the positive electrode side, Li-ions are extracted from the LiFePO$_4$ matrix (Eq. (1)), and the negative reaction is represented by the Zn^{2+} ion reduction/deposition (Eq. (2)) as it was confirmed in this work by observation of operation of a two-electrode beaker cell and reported in our previous works [37]. Upon discharge, Zn metal loses electrons, and dissolves into the electrolyte, while at the positive electrode side, Li-ions intercalate into the FePO$_4$ crystal structure.
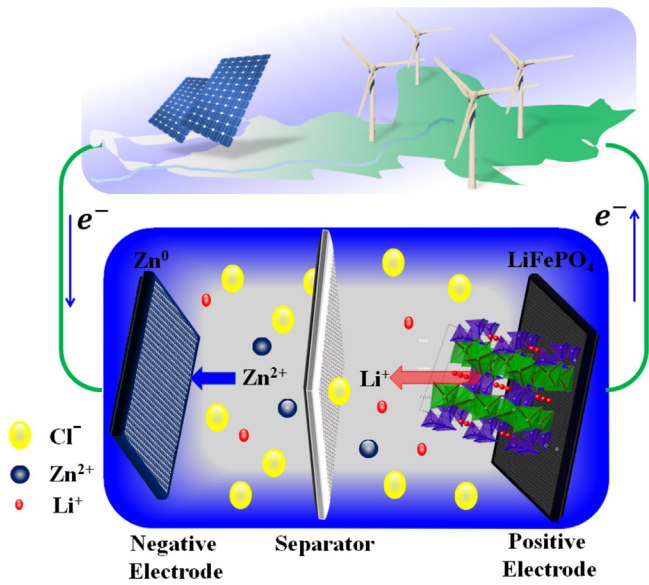
Fig. 4. CV profiles of the battery system at different scan rates from $0.5 \, mV \, s^{-1}$ to $100 \, mV \, s^{-1}$ at different potential ranges.

Fig. 2. Schematics of mechanism of Zn/LiCl-ZnCl$_2$/LiFePO$_4$ aqueous battery during the charge step.

$$LiFePO_4 \leftrightarrow Le^+ + FePO_4 + \bar{e} \tag{1}$$

$$Zn^{2+} + 2\bar{e} \leftrightarrow Zn^0 \tag{2}$$

In contrast with the organic electrolytes in the LIBs, the electrochemical reactions in aqueous media could be complicated by the specific side reactions related to the electrolyte corrosivity, proton co-intercalation and the electrochemical decomposition of water accompanied by the O_2 and H_2 evolution. All these reactions negatively affect the cell reversibility. Therefore, careful selection of electrolyte is crucial to construct a high performance ARLB.
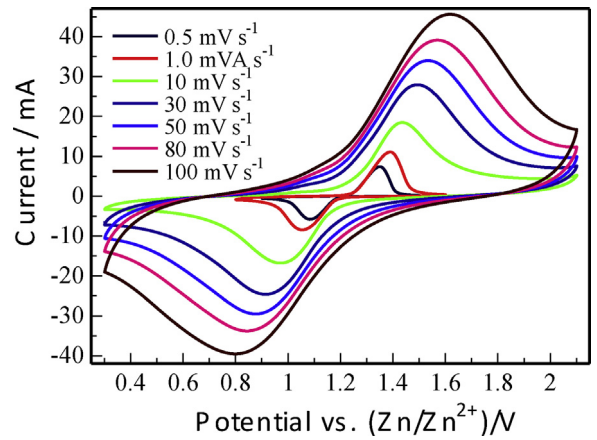
In the Zn/LiFePO$_4$ battery system, the Zn^{2+} ions containing electrolyte is a 'source' of the negative electrode, because during the initial charge, Zn^{2+} ions deposit at the current collector and form the negative electrode. Hence, the concentration of Zn^{2+} in the electrolyte should be high enough to provide sufficient conductivity and sufficient amount of zinc ions for the battery operation. However, the concentration and activity of Zn^{2+} are limited by zinc solubility (K_{sp}) and the electrolyte pH. Hence, as it was suggested in our previous work [37], a binary electrolyte with $3 \, mol \, dm^{-3}$ LiCl and $4 \, mol \, dm^{-3}$ ZnCl$_2$ was prepared as described in experimental section, ensuring high conductivity and sufficient amount of zinc source. It was reported that the redox couple of LiFePO$_4$ is partially reversible as it forms a mixture of LiFePO$_4$ and Fe$_2$O$_3$ in a LiOH electrolyte [38]. Xia's group found that high OH$^-$ concentration can accelerate the cycling fading of LiFePO$_4$ [39]. Hence, an electrolyte with less OH$^-$ (i.e. lower pH) could reduce hydrolysis and improve the electrochemical performance of the
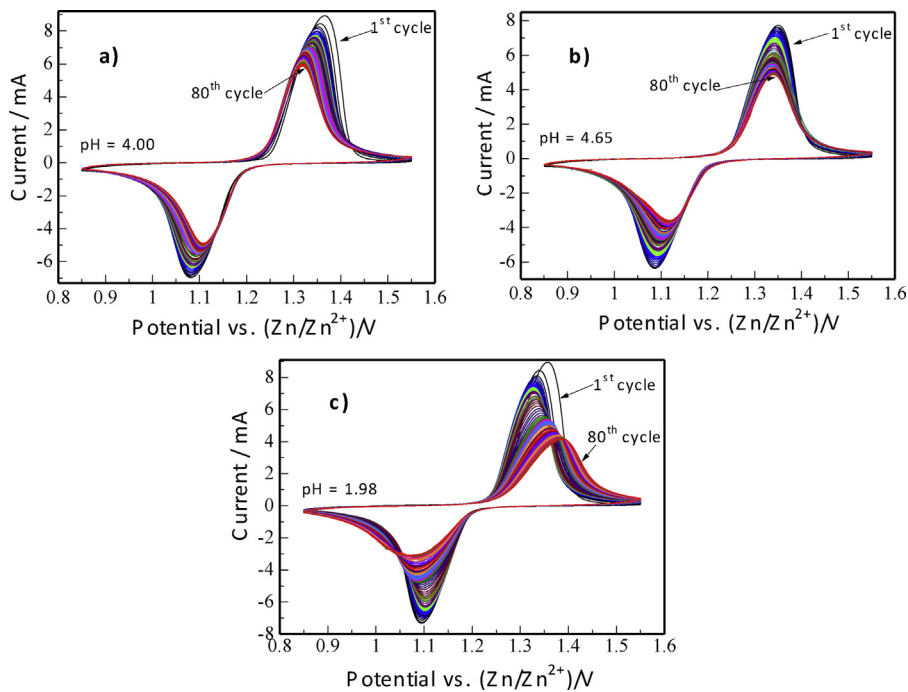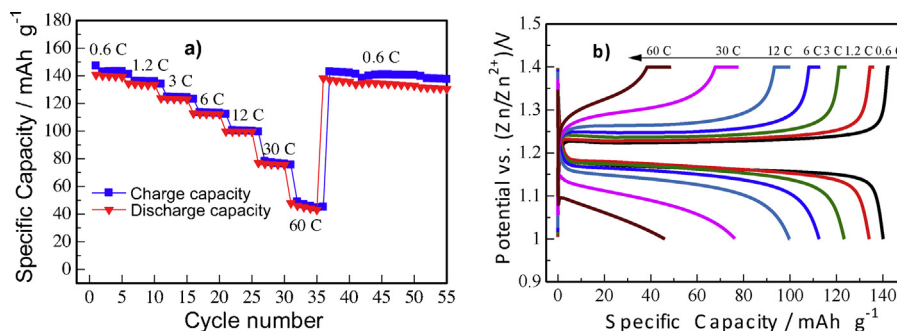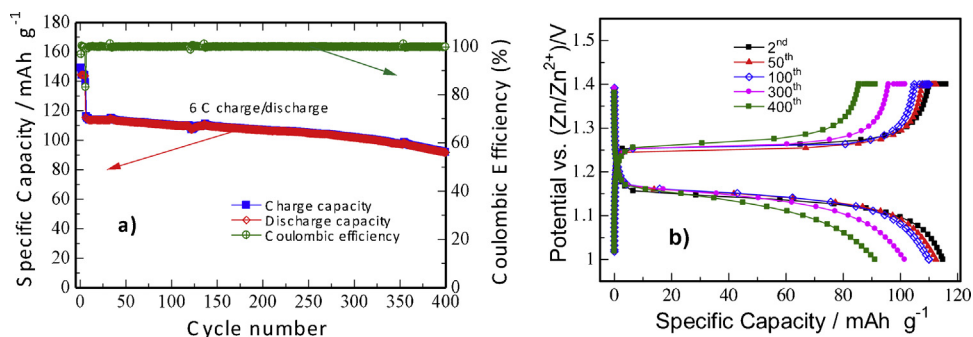

Fig. 3. CVs profiles of Zn/LiFePO$_4$ for 80 cycles, taken at a scan rate of $0.5 \, mV \, s^{-1}$ from 0.9 V to 1.6 V (vs. Zn/Zn^{2+}) at various pH conditions: (a) pH = 4.00; (b) pH = 4.65; (c) pH = 1.98.

Fig. 5. (a) Rate capability of LiFePO$_4$ in the Zn/LiFePO$_4$ battery at various current densities; (b) Charge/Discharge profiles of Zn/LiFePO$_4$ battery at various current densities from 0.6 C to 60 C; cut of voltage 1.0–1.4 V (vs. Zn/Zn^{2+}).

Fig. 6. (a) Cycle performances and coulombic efficiency of LiFePO$_4$ in the Zn/LiFePO$_4$ cell at 6 C (b) Charge/Discharge profiles of Zn/LiFePO$_4$ battery at 2nd, 50th, 100th, 300th and 400th at the current density of 6 C; cut of voltage 1.0–1.4 V (vs. Zn/Zn^{2+}).

cell. However, in a very acidic media, both LiFePO$_4$ and metallic Zn are not stable. Therefore, the electrolyte pH optimization plays crucial role to construct a high performance Zn/LiFePO$_4$ battery. Hence, in this work the effect of pH on the electrochemical performance of Zn/LiFePO$_4$ cell has been systematically investigated. Cyclic voltammetry (CV) tests have been conducted at different pH values (1.98, 4.00, 4.65) as shown in Fig. 3 within a voltage window of 0.9 – 1.6 V (vs. Zn/Zn^{2+}) at 0.5 mV s^{-1} scan rate.

As shown in Fig. 3a (pH = 4), the cell exhibits a single redox couple, which corresponds to the reversible intercalation/deintercalation of Li$^+$ into/from LiFePO$_4$ as it was illustrated in Fig. 2 [40]. From the CV results, cycling performance deteriorates at pH 1.98 and 4.65 as shown in Fig. 3b and Fig. 3c, respectively; it is especially pronounced in highly acidic media (pH = 1.98). Upon cycling the redox peaks broaden and remarkable peaks shifts could be detected in the CV responses of the cell, indicating an

increased polarization effect at pH 1.98 and 4.65. From these results, the optimum pH of the electrolyte was set to 4, and all further experiments were conducted under these optimized conditions.

Fig. 4 shows the CV curves at different scan rates from 0.5 mV s^{-1} to 100 mV s^{-1} at different voltage ranges. It can be seen that the scan rate increase leads to the higher polarization, which is reflected by the increasing separation between reduction and oxidation peaks. However, even at a high scan rate of 100 mV s^{-1}, the redox peaks are well distinguished, suggesting very fast redox kinetics in the proposed electrochemical system.

The electrochemical performance of the LiFePO$_4$ electrode in the battery was further investigated in terms of its rate capability. As shown in Fig. 5a, a high discharge capacity of 141 mAh g^{-1} has been achieved at initial cycle at 0.6 C at room temperature. Although the specific capacity gradually decreases with the current
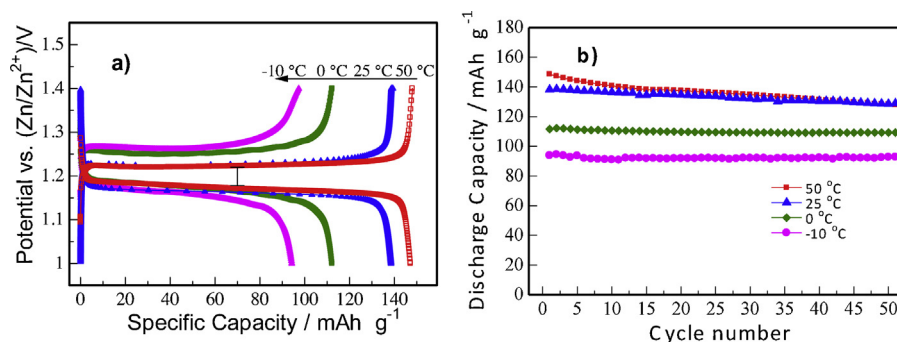
Fig. 7. (a) The 2nd Charge/discharge profiles of LiFePO$_4$ in the Zn/LiFePO$_4$ battery at various temperatures: −10 °C, 0 °C, 25 °C and 50 °C; (b) Discharge capacity versus cycle number of the Zn/LiFePO$_4$ battery charged/discharged at 0.6 C; cut of voltage 1.0–1.4 V (vs. Zn/Zn^{2+}).

Table 1
Electrochemical performance data of Zn/LiFePO$_4$ at various working temperatures

| Working Temperature (°C)	Average Charge/Discharge Potential Difference (V)	Initial Discharge Capacity (mAh g^{-1})	Initial Coulombic Efficiency (%)	Capacity after 50 cycles (mAh g^{-1})	Capacity Retention after 50 cycles (%)
−10	0.10	93.8	66.6	92.7	98.8
−5	0.07	111.7	78.3	109.3	97.9
25	0.06	138.3	95.4	128.7	93.0
50	0.05	148.5	99.0	128.3	86.4

density increase, the capacity is still maintained high and the very high values of 72 mAh g^{-1} and 45 mAh g^{-1} were delivered even at 30 C and 60 C, respectively. Notwithstanding, the capacity is fully recovered when the cycling rate is switched back to 0.6 C, indicating that along with superior rate capability, the Zn/LiCl-ZnCl$_2$/LiFePO$_4$ battery system possesses a very high reversibility and electrochemical stability. The charge/discharge profiles at different current densities are presented in Fig. 5b. The discovered plateaus matched well with the CV results.

Fig. 6a presents the cyclability data of the Zn/LiCl-ZnCl$_2$/LiFePO$_4$ rechargeable battery at 6 C (the initial 5 cycles were conducted at 0.6 C). The cell exhibits a very stable cyclability along with a very high coulombic efficiency (around 100%) over 400 cycles of galvanostatic cycling at 6 C current density (10 minutes for full charge or full discharge based on the theoretical capacity of 170 mAh g^{-1}). A reversible discharge capacity of 107 mAh g^{-1} and 92 mAh g^{-1} were obtained after 200 and 400 cycles, respectively. The charge/discharge profiles at different cycles are shown in Fig. 6b. The potential plateaus maintained without serious distortion upon cycling, which indicates extraordinary cycle performance at high current densities and a prolonged cycle life. The exceptional high performance of the cell was attributed to the

stable performance of LiFePO$_4$ and Zn in the optimized mild acidic aqueous electrolyte.

3.2. Temperature performance of Zn/LiFePO$_4$

The temperature effect on cycling of LiFePO$_4$ in the Zn/LiFePO$_4$ battery was evaluated at a various temperatures from 50 °C to −10 °C at 0.6 C. Fig. 7a shows the 2nd charge/discharge profiles of the cell at different temperatures. The temperature performance data are summarized in Table 1, and it can be seen that by increasing the temperature, the reversible capacity and the initial coulombic efficiency of the cell increase dramatically, and the potential difference between the charge and discharge plateaus reduces, which is due to the increased conductivities and reduced polarization at the higher temperatures. At the lower temperatures, the lithium insertion and extraction reaction are hindered due to their slower kinetics. Furthermore, the electrolyte pH increases with temperature decrease, which results in the lower solubility of Zn^{2+}. Fig. 7b shows the cycling performance of Zn/LiFePO$_4$ battery at different temperatures. At low temperatures −10 °C and 0 °C, the discharge capacities of 92.7 mAh g^{-1} and 109.3 mAh g^{-1} could be achieved, respectively, with extraordinary
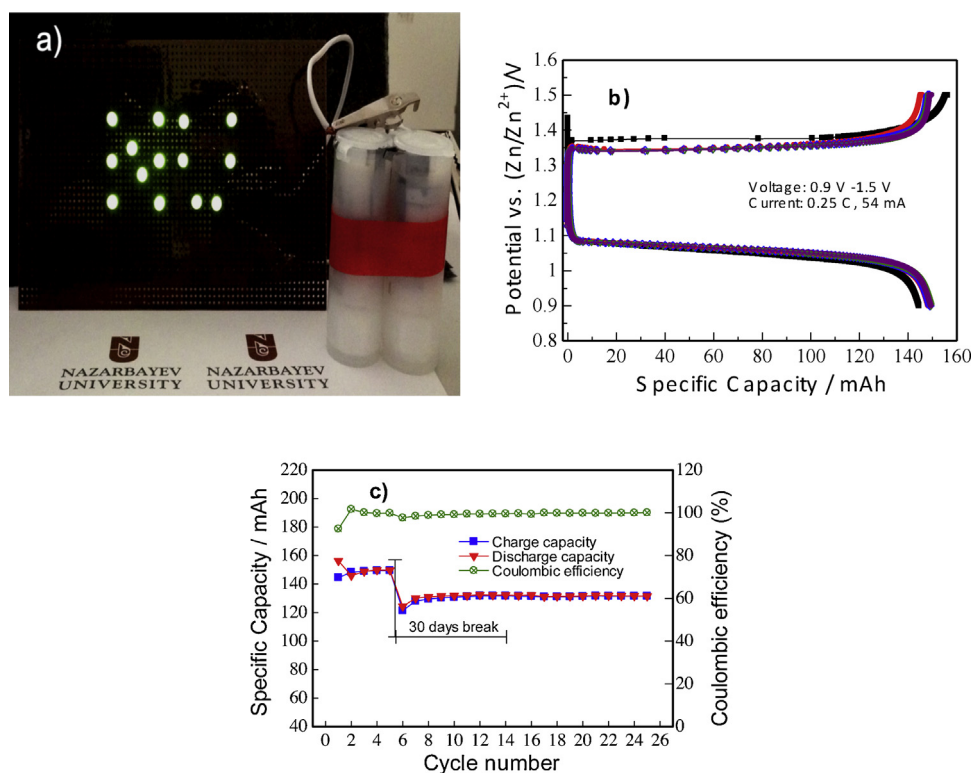
Fig. 8. (a) Two cylindrical large-scale Zn/LiFePO$_4$ batteries with a power capacity of 2.4 V *150 mAh = 0.36 Wh (b) Charge/discharge profiles of a cylindrical large-scale Zn/LiFePO$_4$ battery at 0.25 C from 0.9–1.5 V (vs. Zn/Zn^{2+}); c) Cycle performance of the cylindrical large-scale Zn/LiFePO$_4$ battery at 0.25 C from 0.9–1.5 V (vs. Zn/Zn^{2+}).

capacity retention exceeding 97% over 50 cycles. At 25 °C, the battery delivered the initial discharge capacity of 138.3 mAh g^{-1} with the excellent capacity retention (about 93% as seen from Table 1). At 50 °C, the cell shows a slightly higher capacity of 148.5 mAh g^{-1} due to the higher ionic conductivity and enhanced conditions for the Li-ion diffusion. However, it can be seen that the capacity retention reduces when the cell is cycled at 50 °C. This phenomenon could be due to the lesser stability of both LiFePO$_4$ and metallic zinc in acidic media at high temperatures.

3.3. Large-scale battery design and performances

First time in this work, we assembled a cylindrical large-scale battery of Zn/LiFePO$_4$, as shown in Fig. 8a, and the performance of this system with the LiFePO$_4$ electrode was studied. The mass loading of active material in the cylindrical battery was 1.2 g. The electrode coating area was about 3.5 cm × 13 cm, i.e. the mass loading was almost 264 g m^{-2}, which is much higher than that of the commercial scale electrodes [41]. AGM separator with the thickness of 0.2 mm was used. The 0.1 mm thick zinc foil was used as negative electrode. The carbon paper with positive materials, separator and zinc foil were spirally wounded, and fastened by Teflon® tape. 5 mL of the electrolyte were loaded into a cylindrical cell. After sealing, it was kept for 3 h before further experiments to allow the electrolyte infiltrate into the system. The cylindrical battery was cycled at 54 mA (0.25 C) between voltage 0.9 V to 1.5 V vs. Zn/Zn^{2+}. The cell delivered a capacity of about 150 mAh at the initial five charge/discharge cycles as shown in Fig. 8b. The charge/discharge profiles indicate the polarization increase compared with the small scale Swagelok cells, which is due to the scale-up cell packing techniques and its geometry at current stage: the larger distance between the positive and negative sides increases the cell resistance. The battery was tested for 5 cycles and then rested for 30 days to investigate the capacity retention. After 30 days, the battery was cycled again under the same 54 mA current; the capacity reached 120 mAh at the initial cycle and increased to 130 mAh after 3 cycles and operated without any significant capacity drop during the following 20 cycles as shown in Fig. 8c. Two serial-connected cylindrical cells (2.4 V, 130 mAh) were used to power the LEDs (Parallel connection, L-7113GD 5 mm 2.2 V Green LED 20 micro candela (mcd), Rapid Electronics Ltd.) as shown in Fig. 8a. Furthermore, two cylindrical cells were also used to run an electric car (300 mW) as shown in SI 2 Video 1.

Supplementry material related to this article found, in the online version, at http://dx.doi.org/10.1016/j.electacta.2014.11.168.

Finally, as discovered and reported in this work, the Zn/LiFePO$_4$ full battery with high capacity, and extraordinary rate capability could be practically applicable for large-scale applications. Its performance attributes, compared with the reported performance of various active materials in organic and/or aqueous electrolytes, are evidently attractive and further investigation in the proposed cell configuration concept is very promising. The further work on the negative electrode performance is under consideration to enhance of the energy and cycle life properties of the proposed system. We hope that the results reported here will give strong contribution to the development of ARLBs and increasing the researchers' attention to these systems.

4. Conclusions

A novel Zn/LiFePO$_4$ rechargeable battery with an optimized Li$^+$/Zn^{2+} binary electrolyte has been developed. The commercial lithium iron phosphate (LiFePO$_4$) and Zn metal were chosen as positive and negative electrode, respectively, operating in a mild acidic aqueous electrolyte. It was shown that the choice of the LiFePO$_4$ electrode allows for stable battery functioning, which is due to its operating voltage within the stability window of the electrolyte. The LiFePO$_4$ positive electrode exhibited an excellent cycling performance with a capacity retention of 80% over 400 cycles at 6 C. In addition, the system exhibited an excellent high rate capability up to 60 C. Furthermore, the cell possesses high electrochemical performances at a temperature range from 50 °C and −10 °C, which were attributed to the well optimized positive, negative and electrolyte combination and composition. A cylindrical large-scale battery based on the proposed configuration with a capacity of 150 mAh was successfully designed and first reported. The Zn/LiCl + ZnCl$_2$/LiFePO$_4$ ARLB offers a very promising high safety, low cost, long cycling life, an attractive energy and power densities system for large scale applications.

Acknowledgements

References

[1] P. Simon, Y. Gogotsi, Materials for electrochemical capacitors, Nat. Mater. 7 (2008) 845.

[2] J.M. Tarascon, M. Armand, Review article Issues and challenges facing rechargeable lithium batteries, Nature 414 (2001) 359.

[3] V. Etacheri, R. Marom, R. Elazari, G. Salitra, D. Aurbach, Challenges in the development of advanced Li-ion batteries: a review, Energy Environ. Sci. 4 (2011) 3243.

[4] Z. Gadjourova, Y.G. Andreev, D.P. Tunstall, P.G. Bruce, Ionic conductivity in crystalline polymer electrolytes, Nature 412 (2001) 520.

[5] Z. Stoeva, I. Martin-Litas, E. Staunton, Y.G. Andreev, P.G. Bruce, Ionic conductivity in the crystalline polymer electrolytes PEO$_6$:LiXF$_6$, X = P, As, Sb, J. Am. Chem. Soc. 125 (2003) 4619.

[6] J.Y. Luo, W.J. Cui, P. He, Y.Y. Xia, Raising the cycling stability of aqueous lithium–ion batteries by eliminating oxygen in the electrolyte, Nat. Chem. 2 (2010) 760.

[7] W. Tang, Y.S. Zhu, Y.Y. Hou, L.L. Liu, Y.P. Wu, K.P. Loh, H.P. Zhang, K. Zhu, Aqueous rechargeable lithium batteries as an energy storage system of superfast charging, Energy Environ. Sci. 6 (2013) 2093.

[8] P. He, X. Zhang, Y.G. Wang, L. Cheng, Y.Y. Xia, Lithium-Ion Intercalation Behavior of LiFePO$_4$ in Aqueous and Nonaqueous Electrolyte Solutions, J. Electrochem. Soc. 155 (2008) A144.

[9] Q.T. Qu, L.J. Fu, X.Y. Zhan, D. Samuelis, J. Maier, L. Li, S. Tian, Z.H. Li, Y.P. Wu, Porous LiMn$_2$O$_4$ as cathode material with high power and excellent cycling for aqueous rechargeable lithium batteries, Energy Environ. Sci. 4 (2011) 3985.

[10] R. Ruffo, F. La Mantia, C. Wessells, R.A. Huggins, Y. Cui, Electrochemical characterization of LiCoO$_2$ as rechargeable electrode in aqueous LiNO$_3$ electrolyte, Solid State Ionics 192 (2011) 289.

[11] X.J. Wang, Y.Y. Hou, Y.S. Zhu, Y.P. Wu, R. Holze, An Aqueous Rechargeable Lithium Battery Using Coated Li Metal as Anode, Sci. Reports 3 (2013) 1401.

[12] X.J. Wang, Q.T. Qu, Y.Y. Hou, F.X. Wang, Y.P. Wu, An aqueous rechargeable lithium battery of high energy density based on coated Li metal and LiCoO2, Chem. Commun 49 (2013) 6179.

[13] Y.Y. Hou, X.J. Wang, Y.S. Zhu, C.L. Hu, Z. Chang, Y.P. Wu, R. Holze, Macroporous LiFePO$_4$ as a cathode for an aqueous rechargeable lithium battery of high energy density, J. Mater. Chem. A 1 (2013) 14173.

[14] W. Li, J.R. Dahn, D.S. Wainwright, Rechargeable lithium batteries with aqueous electrolytes, Science 264 (1994) 1115.

[15] J. Kohler, H. Makihara, H. Uegaito, H. Inoue, M. Toki, LiV$_3$O$_8$: characterization as anode material for an aqueous rechargeable Li-ion battery system, Electrochim. Acta 46 (2000) 59.

[16] G.J. Wang, L.J. Fu, N.H. Zhao, L.C. Yang, Y.P. Wu, H.Q. Wu, An Aqueous Rechargeable Lithium Battery with Good Cycling Performance, Angew. Chem., Int. Ed. 46 (2006) 295.

[17] H.B. Wang, K.L. Huang, Y.Q. Zeng, S. Yang, L.Q. Chen, Electrochemical properties of TiP$_2$O$_7$ and LiTi$_2$(PO$_4$)$_3$ as anode material for lithium ion battery with aqueous solution electrolyte, Electrochim. Acta 52 (2007) 3280.

[18] H. Manjunatha, T.V. Venkatesha, G.S. Suresh, Electrochemical studies of LiMnPO$_4$ as aqueous rechargeable lithium–ion battery electrode, J. Solid State Electrochem. 16 (2012) 1941.

[19] J.Y.Y.Y. Luo Xia, Aqueous Lithium-ion Battery LiTi$_2$ (PO$_4$)$_3$/LiMn$_2$O$_4$ with High Power and Energy Densities as well as Superior Cycling Stability, Adv. Funct. Mater. 17 (2007) 3877.

[20] Y.G. Wang, J.Y. Lou, W. Wu, C.X. Wang, Y.Y. Xia, Hybrid Aqueous Energy Storage Cells Using Activated Carbon and Lithium-Ion Intercalated Compounds: III. Capacity Fading Mechanism of LiCo$_{1/3}$Ni$_{1/3}$Mn$_{1/3}$O$_2$ at Different pH Electrolyte Solutions, J. Electrochem. Soc. 154 (2007) A228.

[21] F.X. Wang, S.Y. Xiao, Z. Chang, Y.Q. Yang, Y.P. Wu, Nanoporous LiNi$_{1/3}$Co$_{1/3}$Mn$_{1/3}$O$_2$ as an ultra-fast charge cathode material for aqueous rechargeable lithium batteries, Chem. Commun. 49 (2013) 9209.

[22] C.D. Wessells, R.A. Huggins, Y. Cui, Copper hexacyanoferrate battery electrodes with long cycle life and high power, Nat. Commun. 2 (2011) 550.

[23] C.D. Wessells, S.V. Peddada, R.A. Huggins, Y. Cui, Nickel hexacyanoferrate nanoparticle electrodes for aqueous sodium and potassium ion batteries, Nano Lett. 11 (2011) 5421.

[24] Y. Wang, Y. Wang, E. Hosono, K. Wang, H. Zhou, The Design of a LiFePO$_4$/Carbon Nanocomposite With a Core–Shell Structure and Its Synthesis by an In Situ Polymerization Restriction Method, Angew. Chem. Int. Ed. 47 (2008) 7461.

[25] M. Armand, J.M. Tarascon, Building better batteries, Nature 451 (2008) 652.

[26] F. Sauvage, L. Laffont, J.M. Tarascon, E. Baudrin, Factors affecting the electrochemical reactivity vs. lithium of carbon-free LiFePO$_4$ thin films, J. Power Sources 175 (2008) 495.

[27] X.G. CH. Mi, H.L. Li Zhang, Electrochemical behaviors of solid LiFePO$_4$ and Li$_{0.99}$Nb$_{0.01}$FePO$_4$ in Li$_2$SO$_4$ aqueous electrolyte, J. Electroanal. Chem. 602 (2007) 245.

[28] P. Vanýsek, CRC Handbook of Chemistry and Physics, in: W.M. Haynes (Ed.), 93rd Edition, Chemical Rubber Company Press, USA, 2012.

[29] J.S. Lee, S. Tai Kim, R. Cao, N.-S. Choi, M. Liu, K.T. Lee, J. Cho, Metal–air batteries with high energy density: Li–air versus Zn–air, Adv Energy Mater. 1 (2011) 34.

[30] Y.G. Li, M. Gong, Y.Y. Liang, J. Feng, J.E. Kim, H.L. Wang, G.S. Hong, B. Zhang, H.J. Dai, Advanced zinc-air batteries based on high-performance hybrid electrocatalysts, Nat. Commun. 4 (2013) 1805.

[31] M. Gong, Y. Li, H. Zhang, B. Zhang, W. Zhou, J. Feng, H. Wang, Y. Liang, Z. Fan, J. Liu, H. Dai, Ultrafast high-capacity NiZn battery with NiAlCo-layered double hydroxide, Energy Environ. Sci. 7 (2014) 2025.

[32] ZBB, Energy Corporation, Zinc-Bromine (ZNBR) Flow Battery. http://www.zbbenergy.com/, 1986.

[33] C. Yan, X. Wang, M. Cui, J. Wang, W. Kang, C.Y. Foo, P.S. Lee, Batteries: Stretchable Silver-Zinc Batteries Based on Embedded Nanowire Elastic Conductors, Adv. Energy Mater. 4 (2014), doi:http://dx.doi.org/10.1002/aenm.201470020.

[34] B. Zhang, Y. Liu, X. Wu, Y. Yang, Z. Chang, Z. Wen, Y. Wu, An aqueous rechargeable battery based on zinc anode and Na$_{0.95}$MnO$_2$, Chem. Commun. 50 (2014) 1209.

[35] K. Takegami, N. Furuya, Aqueous lithium ion–Zinc secondary battery, Electrochemistry 74 (2006) 825.

[36] H. Zhang, Q. Du, C. Li, X. Sun, Binary Ion Batteries Operating on the Model of Newton's Cradle, J. Electrochem. Soc. 159 (2012) A2001–A2004.

[37] J. Yan, J. Wang, H. Liu, Z. Bakenov, D. Gosselink, P. Chen, Rechargeable hybrid aqueous batteries, J. Power Sources 216 (2012) 222.

[38] M. Manickama, P. Singha, S. Thurgatea, K. Prince, Redox behavior and surface characterization of LiFePO$_4$ in lithium hydroxide electrolyte, J. Power Sources 158 (2006) 646.

[39] P. He, J.L. Liu, W.J. Cui, J.Y. Luo, Y.Y. Xia, Investigation on capacity fading of LiFePO$_4$ in aqueous electrolyte, Electrochim. Acta 56 (2011) 2351.

[40] H. Zhang, X. Wu, T. Yang, S. Liang, X. Yang, Cooperation behavior between heterogeneous cations in hybrid batteries, Chem. Commun. 49 (2013) 9977.

[41] D. Aurbach, B. Markovsky, A. Rodkin, M. Cojocaru, E. Levi, H.J. Kim, An analysis of rechargeable lithium-ion batteries after prolonged cycling, Electrochim. Acta 47 (2002) 1899.